1-1-2009

Carbon–Phosphorus Bond Activation of Tri(2-thienyl)phosphine at Dirhenium and Dimanganese Centers

Md. Nazim Uddin
Jahangirnagar University

M. Abdul Mottalib
Lund University

Noorjahan Begum
Lund University

Shishir Ghosh
Jahangirnagar University

Arun K. Raha
Jahangirnagar University

See next page for additional authors

Accepted version. *Organometallics*, Vol. 28, No. 5 (2009): 1514-1523. DOI.

Organometallics, Vol. 28, No. 5 (2009): 1514-1523. DOI.

Carbon–Phosphorus Bond Activation of Tri(2-thienyl)phosphine at Dirhenium and Dimanganese Centers

Md. Nazim Uddin
Department of Chemistry, Jahangirnagar University, Savar, Bangladesh
M. Abdul Mottalib
Inorganic Chemistry Research Group, Chemical Physics, Center for Chemistry and Chemical Engineering, Lund University, Lund, Sweden
Noorjahan Begum
Inorganic Chemistry Research Group, Chemical Physics, Center for Chemistry and Chemical Engineering, Lund University, Lund, Sweden
Shishir Ghosh
Department of Chemistry, Jahangirnagar University, Savar, Bangladesh
Arun K. Raha
Department of Chemistry, Jahangirnagar University, Savar, Bangladesh

Daniel T. Haworth
Department of Chemistry, Marquette University, Milwaukee, Wisconsin
Sergey V. Lindeman
Department of Chemistry, Marquette University, Milwaukee, Wisconsin
Tasneem A. Siddiquee
Department of Chemistry, University of Wisconsin−Milwaukee, Milwaukee, Wisconsin
Dennis W. Bennett
Department of Chemistry, University of Wisconsin−Milwaukee, Milwaukee, Wisconsin
Graeme Hogarth
Department of Chemistry, University College London, London, U.K.
Ebbe Nprdlander
Inorganic Chemistry Research Group, Chemical Physics, Center for Chemistry and Chemical Engineering, Lund University, Lund, Sweden
Shariff E. Kabir
Department of Chemistry, Jahangirnagar University, Savar, Dhaka-1342, Bangladesh

Synopsis

Reactions of the dirhenium and dimanganese complexes $[Re_2(CO)_{10-x}(NCMe)_x]$ (x = 0, 1, 2) and $[Mn_2(CO)_{10}]$ with tri(2-thienyl)phosphine in different conditions are studied. A variety of mono- and dinuclear complexes are obtained from these reactions by C—P bond cleavage of the tri(2-thienyl)phosphine ligand.

Abstract

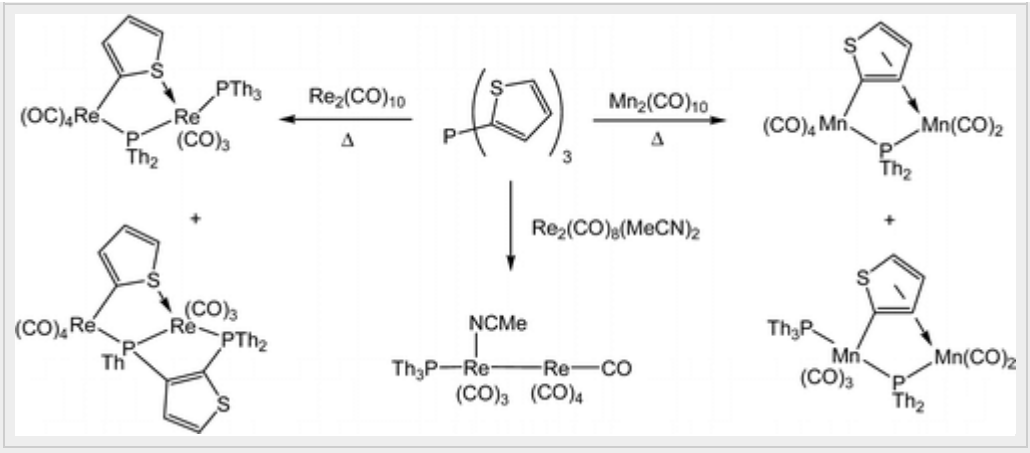

Reaction of $[Re_2(CO)_9(NCMe)]$ with tri(2-thienyl)phosphine (PTh_3) in refluxing cyclohexane affords three substituted dirhenium complexes: $[Re_2(CO)_9(PTh_3)]$ (**1**), $[Re_2(CO)_8(NCMe)(PTh_3)]$ (**2**), and $[Re_2(CO)_8(PTh_3)_2]$ (**3**). Complex **2** was also obtained from the room-temperature reaction of $[Re_2(CO)_8(NCMe)_2]$ with PTh_3 and is an unusual example in which the acetonitrile and phosphine ligands are coordinated to the same rhenium atom. Thermolysis of **1** and **3** in refluxing xylene affords

$[Re_2(CO)_8(\mu\text{-}PTh_2)(\mu\text{-}\eta^1{:}\kappa^1\text{-}C_4H_3S)]$ (**4**) and $[Re_2(CO)_7(PTh_3)(\mu\text{-}PTh_2)(\mu\text{-}H)]$ (**5**), respectively, both resulting from carbon−phosphorus bond cleavage of a coordinated PTh_3 ligand. Reaction of $[Re_2(CO)_{10}]$ and PTh_3 in refluxing xylene gives a complex mixture of products. These products include **3**–**5**, two further binuclear products, $[Re_2(CO)_7(PTh_3)(\mu\text{-}PTh_2)(\mu\text{-}\eta^1{:}\kappa^1\text{-}C_4H_3S)]$ (**6**) and $[Re_2(CO)_7(\mu\text{-}\kappa^1{:}\kappa^2\text{-}Th_2PC_4H_2SPTh)(\mu\text{-}\eta^1{:}\kappa^1\text{-}C_4H_3S)]$ (**7**), and the mononuclear hydrides $[ReH(CO)_4(PTh_3)]$ (**8**) and *trans*-$[ReH(CO)_3(PTh_3)_2]$ (**9**). Binuclear **6** is structurally similar to **4** and can be obtained from reaction of the latter with 1 equiv of PTh_3. Formation of **7** involves a series of rearrangements resulting in the formation of a unique new diphosphine ligand, $Th_2PC_4H_2SPTh$. Reaction of $[Mn_2(CO)_{10}]$ with PTh_3 in refluxing toluene affords the phosphine-substituted product $[Mn_2(CO)_9(PTh_3)]$ (**10**) and two carbon−phosphorus bond cleavage products, $[Mn_2(CO)_6(\mu\text{-}PTh_2)(\mu\text{-}\eta^1{:}\eta^5\text{-}C_4H_3S)]$ (**11**) and $[Mn_2(CO)_5(PTh_3)(\mu\text{-}PTh_2)(\mu\text{-}\eta^1{:}\eta^5\text{-}C_4H_3S)]$ (**12**). Both **11** and **12** contain a bridging thienyl ligand that is bonded to one manganese atom in a η^5-fashion. The molecular structures of eight of these new complexes were established by single-crystal X-ray diffraction studies, allowing a detailed analysis of the disposition of the coordinated ligands.

Introduction

The removal of organosulfur compounds from liquid fuels is important for both industrial and environmental reasons.[1,2] They are found in a variety of species such as thiols, thioethers, disulfides, and thiophenes, and total amounts range from 0.2 to 4% in crude petroleum.[3,4] Sulfur is currently removed from petroleum feedstocks using a catalytic process known as hydrodesulfurization (HDS). This large-scale process is typically performed at high H_2 pressures and temperatures in the presence of sulfided metal-based catalysts such as Ni- and Co-promoted MoS_2 and WS_2 supported on alumina.[1,4,5] Of the sulfur impurities present in crude petroleum, thiophenes are among the most resistant toward HDS due to aromatic stabilization of the thiophene ring.[5,6] Several other metal sulfides, MS_x (M = Ru, Re, Os, Rh, and Ir), have shown higher catalytic activities for the desulfurization of thiophenes under various hydrotreating conditions[7,8] among which the second-row (such as Ru and Rh) and third-row (such as Re, Os, and Ir) elements have been proven to be the most active catalysts, but high costs prevent their commercial use.[4]

Table 1. Crystallographic Data and Structure Refinement for 2, 3, 5, and 6

	2	3	5	6
empirical formula	$C_{22}H_{12}NO_8PRe_2S_3$	$C_{32}H_{18}O_8P_2Re_2S_6$	$C_{27}H_{16}O_7P_2Re_2S_5$	$C_{31}H_{18}O_7P_2Re_2S_6$
fw	917.88	1157.16	1047.04	1129.15
temp (K)	100(2)	100(2)	100(2)	100(2)

	2	3	5	6
wavelength (Å)	1.54178	1.54178	1.54178	1.54178
cryst syst	monoclinic	monoclinic	monoclinic	monoclinic
space group	$P2_1/c$	$P2_1/c$	$P2_1/n$	$P2_1/c$
a (Å)	18.8163(3)	15.7678(3)	13.1837(2)	17.2981(3)
b (Å)	8.5529(2)	14.9874(2)	11.2234(2)	11.5799(2)
c (Å)	17.8091(3)	15.3262(3)	22.1690(4)	17.6625(3)
α (deg)	90	90	90	90
β (deg)	111.886(1)	93.1750(1)	104.315(1)	99.369(1)
γ (deg)	90	90	90	90
volume (Å^3)	2659.52(9)	3616.30(1)	3178.41(9)	3490.8(1)
Z	4	4	4	4
D_{calc} (Mg m^{-3})	2.292	2.125	2.188	2.149
μ(Mo Kα) (mm^{-1})	20.723	17.399	19.076	17.980
F(000)	1712	2200	1976	2144
cryst size (mm)	0.40 × 0.20 × 0.07	0.38 × 0.18 × 0.11	0.42 × 0.20 × 0.09	0.30 × 0.17 × 0.12
θ range (deg)	2.53−61.43	4.07−61.50	3.56−61.52	2.59−67.35

	2	3	5	6
limiting indices	$-21 \le h \ge 19$,	$-17 \le h \ge 17$,	$-15 \le h \ge 14$,	$-20 \le h \ge 19$,
	$0 \le k \ge 9$,	$0 \le k \ge 16$,	$0 \le k \ge 12$,	$0 \le k \ge 13$,
	$0 \le l \ge 20$	$0 \le l \ge 17$	$0 \le l \ge 24$	$0 \le l \ge 21$
reflns collected	19 415	29 928	26 344	29 272
indep reflns (R_{int})	3979 (0.0303)	5492 (0.0246)	4846 (0.0271)	5919 (0.0410)
max. and min. transmn	0.3249 and 0.0442	0.2506 and 0.0580	0.2786 and 0.0460	0.2215 and 0.0747
data/restraints/params	3979/150/344	5492/100/465	4846/360/386	5919/222/367
goodness of fit on F^2	1.277	1.240	1.328	1.064
final R indices [$I > 2\sigma(I)$]	$R_1 = 0.0249$,	$R_1 = 0.0185$,	$R_1 = 0.0195$,	$R_1 = 0.0256$,
	$wR_2 = 0.0572$	$wR_2 = 0.0444$	$wR_2 = 0.0466$	$wR_2 = 0.0568$
R indices (all data)	$R_1 = 0.0257$,	$R_1 = 0.0186$,	$R_1 = 0.0196$,	$R_1 = 0.0289$,
	$wR_2 = 0.0575$	$wR_2 = 0.0445$	$wR_2 = 0.0466$	$wR_2 = 0.0582$
largest diff in peak and hole ($Å^{-3}$)	e1.172 and −0.604	0.865 and −0.636	0.699 and −0.646	1.088 and −0.638

Table 2. Crystallographic Data and Structure Refinement for 7, 9, 11, and 12

	7	9	11	12
empirical formula	$C_{27}H_{14}O_7P_2Re_2S_5$	$C_{27}H_{19}O_3P_2ReS_6$	$C_{18}H_9Mn_2O_6PS_3$	$C_{29}H_{18}Mn_2O_5P_2S_6$
fw	1045.02	831.92	558.28	810.61
temp (K)	100(2)	293(2)	100(2)	100(2)
wavelength (Å)	1.54178	0.71073	1.54178	1.54178
cryst syst	monoclinic	monoclinic	monoclinic	monoclinic
space group	*C*2/*c*	C_2	$P2_1/n$	$P2_1/c$
a (Å)	10.3510(2)	16.942(1)	15.8855(3)	17.5628(3)
b (Å)	17.8149(4)	9.1677(6)	9.0020(1)	11.8433(2)
c (Å)	33.7373(7)	10.0865(7)	16.0108(3)	16.8854(3)
α (deg)	90	90	90	90
β (deg)	96.734(1)	100.868(1)	113.929(1)	116.495(1)
γ (deg)	90	90	90	90
volume ($Å^3$)	6178.3(2)	1538.5(2)	2092.77(6)	3143.31(9)
Z	8	2	4	4
D_{calc} (Mg m^{-3})	2.247	1.796	1.772	1.713

	7	9	11	12
μ(Mo Kα) (mm^{-1})	19.627	4.489	13.654	11.570
F(000)	3936	812	1112	1632
cryst size (mm)	0.24 × 0.22 × 0.20	0.59 × 0.37 × 0.13	0.50 × 0.24 × 0.17	0.38 × 0.18 × 0.18
θ range (deg)	2.64−61.74	2.06−28.26	3.31−61.49	2.81−61.50
limiting indices	−11 ≤ *h* ≥ 11,	−22 ≤ *h* ≥ 22,	−17 ≤ *h* ≤ 16,	−19 ≤ *h* ≤ 17,
	0 ≤ *k* ≥ 19,	−11 ≤ *k* ≥ 11,	0 ≤ *k* ≤ 10,	0 ≤ *k* ≤ 13,
	0 ≤ *l* ≥ 37	−12 ≤ *l* ≥ 13	0 ≤ *1* ≤ 18	0 ≤ *1* ≤ 18
reflns collected	26 027	6795	17 370	26 288
indep reflns (R_{int})	4673 (0.0243)	3443 (0.0129)	3137 (0.0328)	4792 (0.0271)
max. and min. transmn	0.1109 and 0.0884	0.5845 and 0.1760	0.2049 and 0.0558	0.2299 and 0.0964
data/restraints/params	4673/160/429	3443/2/169	3137/0/313	4792/360/475
goodness of fit on F^2	1.326	1.094	1.038	1.061
final *R* indices [$I > 2\sigma(I)$]	R_1 = 0.0215,	R_1 = 0.0412,	R_1 = 0.0226,	R_1 = 0.0273,
	wR_2 = 0.0514	wR_2 = 0.1132	wR_2 = 0.0544	wR_2 = 0.0654
R indices (all data)	R_1 = 0.0215,	R_1 = 0.0413,	R_1 = 0.0235,	R_1 = 0.0289,

	7	9	11	12
	wR_2 = 0.0514	wR_2 = 0.01133	wR_2 = 0.0548	wR_2 = 0.0662
largest diff in peak and hole (e0.816 and −0.476	1.389 and −1.567	0.347 and −0.258	0.364 and −0.335 Å^{-3})	

A variety of organometallic systems, including transition-metal clusters, have been studied as models for the catalytic HDS of thiophenes since mechanistic information can be easily obtained by spectroscopic and analytical studies of discrete molecular complexes.[9-12] As a consequence, a thorough investigation of the reactivity of thiophenes toward transition metal centers has been studied by several groups as models of thiophene adsorption on HDS catalysts. These have been the subject of reviews, although the interaction of thiophenes with the catalyst surface during HDS is not yet properly understood.[1,4,8-21] On the basis of these studies, it has been proposed that substrate binding to active metal sites through the sulfur atom is an initial step followed by carbon−sulfur bond cleavage.[17a,21]

Numerous examples of thiophene coordination and activation have been reported from which it is clear that thiophene is a relatively poor ligand for low-valent metal complexes. To overcome this difficulty, heterodifunctional phosphines such as diphenyl(2-thienyl)phosphine, phenyldi(2-thienyl)phosphine, and tri(2-thienyl)phosphine, capable of introducing the thienyl, C_4H_3S, ligand as a result of carbon−phosphorus bond cleavage, have been widely studied.[22-27] Estevan et al. obtained only carbon−hydrogen bond cleavage products with rhodium complexes,[28] while both carbon−hydrogen and carbon−phosphorus bond cleavage were observed at osmium and ruthenium centers.[24-26] The coordination of a sulfur atom of the thienyl ring to a metal center, which is required for desulfurization, is rarely observed for osmium and ruthenium complexes. In contrast, sulfur coordination is frequently observed for group seven metal carbonyls.[23] For example, Deeming et al. reported the synthesis of $[Re_2(CO)_8(\mu\text{-}\kappa^1\text{:}\kappa^1\text{-}Ph_2PC_4H_3S)]$ (**A**, Chart 1), obtained from the photochemical reaction between $[Re_2(CO)_{10}]$ and diphenyl(2-thienyl)phosphines, while $[Re_2(CO)_8(\mu\text{-}PPh_2)(\mu\text{-}\eta^1\text{:}\kappa^1\text{-}Ph_2PC_4H_3S)]$ (**B**) results when the same reactants are heated in xylene. Significantly, both contain a rhenium−sulfur bond (Chart 1).[23]With $[Mn_2(CO)_{10}]$ the reaction takes a different course, and $[Mn_2(CO)_9\{PPh_2(C_4H_3S)\}]$ (**C**) and $[Mn_2(CO)_6(\mu\text{-}PPh_2)(\mu\text{-}\eta^1\text{:}\eta^5\text{-}C_4H_3S)]$ (**D**) are both formed from the reaction with diphenyl(2-thienyl)phosphine in refluxing xylene (cf. Chart 1).[23] The latter is of particular interest since the generated thienyl ligand acts as a net seven-electron donor to the dimanganese unit. In both of these examples, while metal−sulfur bonds are readily formed, no evidence of carbon−sulfur bond cleavage is noted, a reaction clearly important in the

desulfurization process. In related work, however, we have recently reported both carbon−hydrogen bond activation and carbon−sulfur bond scission of a coordinated PTh_3 ligand on a triruthenium cluster, resulting in the formation of a μ_3-η^3-1-thiabutadiene ligand.[27]

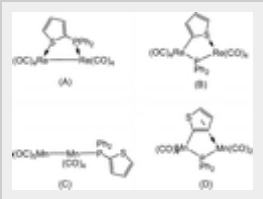

Chart 1

As a part of our work on the reactivity of heterodifunctional ligands with transition metal complexes, we have investigated the reaction of PTh_3 toward dirhenium and dimanganese carbonyls since surprisingly little is known about its coordination behavior with group 7 metals. Herein we report the unexpected reactivity of this ligand toward rhenium carbonyl complexes, giving rise to mono- and binuclear complexes. Surprisingly, the latter consists of thienyl, phosphido, and diphosphine ligands arising from carbon−phosphorus bond cleavage as well as later carbon−phosphorus bond formation of the activated ligands.

Results and Discussion

(i) Reaction of $[Re_2(CO)_9(NCMe)]$ with PTh_3: Formation of Substitution Complexes

Heating $[Re_2(CO)_9(NCMe)]$ and PTh_3 in refluxing cyclohexane affords after workup three substituted dirhenium complexes, $[Re_2(CO)_9(PTh_3)]$ (**1**), $[Re_2(CO)_8(NCMe)(PTh_3)]$ (**2**), and $[Re_2(CO)_8(PTh_3)_2]$ (**3**), in 28, 54, and 12% yields, respectively (Scheme 1). In separate experiments, **2** was shown to be a precursor to **3**, while **2** was also obtained upon addition of equimolar amounts of $[Re_2(CO)_8(NCMe)_2]$ and PTh_3 at room temperature or upon treatment of an acetonitrile solution of **1** with Me_3NO under the same conditions.

Scheme 1

We were unable to obtain single crystals of **1**, but its molecular structure is readily assigned from spectroscopic data. The carbonyl region of the IR spectrum is very similar to those of other

monosubstituted compounds $[Re_2(CO)_9L]$ (L = ^tBuNC, PBz_3, RCN),[29-31] and the FAB mass spectrum shows a parent molecular ion peak at *m/z* 904 together with other ions due to the sequential loss of each of nine carbonyls. The $^{31}P\{^1H\}$ NMR spectrum shows a singlet at δ −24.5, while the ^1H NMR spectrum has three equal intensity multiplets at δ 7.64, 7.35, and 7.22 assigned to the thienyl-ring protons.

Spectroscopic data for **2** are similar to those described for **1**. The $^{31}P\{^1H\}$ NMR spectrum again shows only a singlet at δ −23.6, while the ^1H NMR spectrum displays three multiplets at δ 7.60, 7.42, and 7.19 assigned to the PTh_3 ligand and a singlet at δ 2.0 attributed to the methyl protons of the acetonitrile group. These four signals are in a 1:1:1:1 ratio, suggesting equivalent numbers of phosphine and acetonitrile ligands. The FAB mass spectrum shows a parent molecular ion at *m/z* 917 and fragmentation peaks due to the sequential loss of the acetonitrile and eight CO groups. On the basis of the spectroscopic data alone it was not possible to unambiguously assign the relative positions of the substituted ligands, and hence a single-crystal X-ray diffraction study was carried out, the result of which is shown in Figure 1. The most striking feature is the coordination of both the phosphine and acetonitrile ligands to the same rhenium atom, phosphine being axially coordinated, while the acetonitrile occupies an equatorial site. The structure is similar to that of $[Re_2(CO)_{10}]$,[32] with two staggered square-pyramidal ReL_5 groups being joined by a single rhenium−rhenium bond [Re(1)—Re(2) 3.0245(3) Å]. The rhenium−phosphorus bond distance [Re(2)—P(1) 2.3388(13) Å] is somewhat shorter than those in the literature,[23,33,34] while the rhenium−nitrogen distance [Re(2)—N(1) 2.145(4) Å] is within the range reported for related compounds.[35-38]

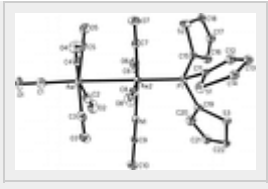

Figure 1. ORTEP diagram of the molecular structure of $[Re_2(CO)_8(NCMe)(PTh_3)]$ (**2**), showing 50% probability thermal ellipsoids. Selected interatomic distances (Å) and angles (deg): Re(1)—Re(2) 3.0245(3), Re(2)—N(1) 2.145(4), Re(2)—P(1) 2.338(1), av Re—C 1.978(6), av C—O 1.143(7), P(1)—Re(2)—Re(1) 175.86(3), N(1)—Re(2)—Re(1) 86.3(1), N(1)—Re(2)—P(1) 92.5(1), C(8)—Re(2)—N(1) 89.8(2), C(7)—Re(2)—N(1) 175.2(2), C(1)—Re(1)—Re(2) 177.5(2), C(4)—Re(1)—C(3) 90.9(2), C(5)—Re(1)—C(3) 169.0(2).

As far as we are aware, this is only the second crystallographically characterized $[Re_2(CO)_8L_2]$ complex in which both substituents are bound to the same metal atom. The previous example of another complex of this type (**E**, Chart 2) was reported by Adams et al. in 8% when the 2,6-isomer was exposed to fluorescent light.[30] Ingham and Colville have previously reported the

synthesis of $[Re_2(CO)_8(NCMe)(PBz_3)]$ (**F**) upon treatment of axial-$[Re_2(CO)_9(PBz_3)]$ with Me_3NO in MeCN.[29] On the basis of spectroscopic data it was proposed to exist entirely in a single isomeric form in which the phosphine occupied an axial site on one metal and the MeCN an equatorial site at the other (i.e., a 1,6-isomer, Chart 2). This assignment was made primarily on the basis of the carbonyl region of the IR spectrum in hexane, 2074w, 2026sh, 2012m, 1974vs, 1927s, and 1914m cm^{-1}, which may be compared to that of **2** in CH_2Cl_2, 2087s, 2002m, 1977vs, 1949m, and 1917m cm^{-1}. While the two are in different solvents, it is clear from their form that they represent different isomeric forms. The reason for this is unclear; however, we note that **F** was prepared at room temperature, while **2** was formed at 80 °C. The higher temperature of the latter reaction potentially allows for a secondary isomerization to occur. This can also be rationalized in terms of the *cis*-effect; that is, the coordinatively unsaturated intermediate formed after the dissociation of CO is stabilized by the η^2-coordination mode of the adjacent MeCN ligand, since complex **2** is obtained in more than 40% yield. Interestingly, when **2** was prepared from $[Re_2(CO)_8(NCMe)_2]$ (**G**), the reaction was carried out at room temperature and the same ligand arrangement was obtained. The bis(acetonitrile) complex is known to exist as a 2:1 mixture of 2,6- and 2,3-isomers, which are in equilibrium (Chart 2).[29] Importantly, in both, the MeCN groups always occupy equatorial sites. Addition of PTh_3 to $[Re_2(CO)_8(NCMe)_2]$ possibly leads to a selective reaction with the minor 2,3-isomer to give the observed product after ligand redistribution at the substituted metal center, with concomitant shift of the equilibrium.

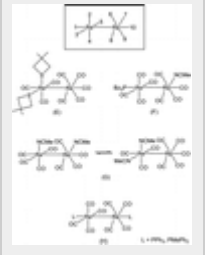

Chart 2

The carbonyl region of the IR spectrum of **3** is indicative of a $[Re_2(CO)_8L_2]$[29-31] complex, and the FAB mass spectrum shows a parent molecular ion peak at *m/z* 1158 together with fragmentation peaks due to the stepwise loss of all eight carbonyl groups. A singlet in the $^{31}P\{^1H\}$ NMR spectrum at δ −23.5 shows that the two phosphines are equivalent and, thus, suggests an axially disubstituted product. This was confirmed by an X-ray crystallographic study, the result of which is summarized in Figure 2. The rhenium−rhenium [Re(1)—Re(2) 3.0442(2) Å] and rhenium−phosphorus [Re(1)—P(1) 2.3410(9) Å and Re(2)—P(2) 2.3553(9) Å] bond distances are consistent with those seen in **2**. The two phosphines occupy axial sites at different metal atoms (i.e., a 1,10-isomer), and in this respect the structure is closely related to that of

$[Re_2(CO)_8L_2]$ (**H**, L = $PMePh_2$, PPh_3), which also adopts a similar diaxial conformation (Chart 2).[31b] Formation of **3** from **2** is superficially simple; however, on closer inspection it necessitates the transfer of one ligand (either CO, MeCN, or phosphine) from one metal atom to the second. We favor a process whereby initial substitution of acetonitrile affords the less stable axial−equatorial 1,2-isomer, and this subsequently rearranges to afford the thermodynamically preferred 1,10-dixial isomer. In other work, transformation of bis(phosphine) complexes $[Re_2(CO)_8L_2]$ from the initially formed axial−equatorial 1,6-isomers into the diaxial 1,10-isomer has been shown to occur only upon prolonged thermolysis.(39) Formation of **3** from **2** occurs at room temperature, and hence the direct formation of a 1,6-isomer is highly unlikely.

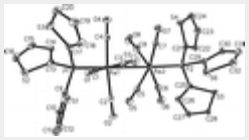

Figure 2. ORTEP diagram of the molecular structure of $[Re_2(CO)_8(PTh_3)_2]$ (**3**), showing 50% probability thermal ellipsoids. Selected interatomic distances (Å) and angles (deg): Re(1)—Re(2) 3.0442(2), Re(1)—P(1) 2.3410(9), Re(2)—P(2) 2.3553(9), av Re—C 1.989(4), av C—O 1.140(5), P(1)—Re(1)—Re(2) 177.15(2), P(2)—Re(2)—Re(1) 174.75(2), C(4)—Re(1)—C(3) 90.2(2), C(4)—Re(1)—C(2) 172.8(2), C(4)—Re(1)—P(1) 94.0(1), C(4)—Re(1)—Re(2) 86.0(1), C(6)—Re(2)—C(5) 88.29(15), C(6)—Re(2)—C(8) 169.4(2), C(6)—Re(2)—P(2) 94.5(1), C(6)—Re(2)—Re(1) 82.6(1).

(ii) Carbon−Phosphorus Bond Activation of a Coordinated PTh_3 Ligand

In an attempt to generate metal-bound thienyl ligands, we investigated the thermal stability of **1**and **3**. Heating **1** in refluxing xylene resulted in formation of $[Re_2(CO)_8(\mu\text{-}PTh_2)(\mu\text{-}\eta^1{:}\kappa^1\text{-}C_4H_3S)]$ (**4**) in 35% yield (Scheme 2). This results from loss of one carbonyl and oxidative addition of a carbon−phosphorus bond to the dirhenium center. The spectroscopic data show that it is a direct analogue of **B** (Chart 1). The IR spectra are virtually the same, and the $^{31}P\{^1H\}$ NMR spectrum consists only of a singlet at δ −58.2. The FAB mass spectrum shows a parent molecular ion at *m*/*z*876 together with ions due to sequential loss of eight carbonyl groups. Formation of **4** upon heating **1** contrasts with the thermal rearrangement of $[Re_2(CO)_9(PPh_3)]$, which affords $[Re_2(CO)_8(\mu\text{-}PPh_2)(\mu\text{-}H)]$.[40]

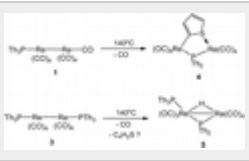

Scheme 2

In contrast, heating **3** in xylene afforded [$Re_2(CO)_7(PTh_3)(\mu\text{-}PTh_2)(\mu\text{-}H)$] (**5**) in 50% yield. Formation of a bridging hydride was immediately apparent from the ^1H NMR spectrum, which contains a doublet of doublets at δ −13.83 (J = 16.4, 5.2 Hz), while the $^{31}P\{^1H\}$ NMR spectrum consists of a pair of doublets at δ −8.3 and −28.4 (J_{PP} = 78.8 Hz). In order to fully elucidate the structure, an X-ray crystal structure was carried out, the result of which is summarized in Figure 3. The molecule consists of a dirhenium core with seven terminal carbonyl ligands, an intact PTh_3ligand, a bridging hydride (located and refined in the structural analysis, Re(1)—H(1H) 1.7809, Re(2)—H(1H) 2.0027 Å), and a bridging di(2-thienyl)phosphido moiety. The PTh_3 ligand occupies an equatorial site and lies *trans* to the phosphido bridge [P(1)—Re(2)—P(2) 164.84(3)°]. The structure closely resembles that of [$Re_2(CO)_7(PPh_3)(\mu\text{-}PPh_2)(\mu\text{-}H)$], obtained as one of six products upon heating [$Re_2(CO)_8(PPh_3)_2$] in xylene at 180−230 °C.[40] The rhenium−rhenium bond length in **5** of 3.1555(2) Å is consistent with values reported for other hydride-bridged rhenium−rhenium single bonds. Formation of **5** involves cleavage of a phosphorus−carbon bond and abstraction of a hydride from xylene (most likely), although we have no evidence for the latter.

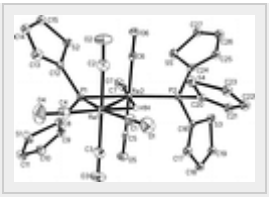

Figure 3. ORTEP diagram of the molecular structure of [$Re_2(CO)_7(PTh_3)(\mu\text{-}PTh_2)(\mu\text{-}H)$] (**5**), showing 50% probability thermal ellipsoids. Selected interatomic distances (Å) and angles (deg): Re(1)—Re(2) 3.1555(2), Re(1)—P(1) 2.433(1), Re(2)—P(1) 2.3970(9), Re(2)—P(2) 2.4097(9), Re(1)—H(1H) 1.7809, Re(2)—H(1H) 2.0027, av Re—C 1.974(5), av C—O 1.138(5), P(1)—Re(1)—Re(2) 48.72(2), P(1)—Re(2)—Re(1) 49.71(2), Re(1)—P(1)—Re(2) 81.58(3), P(2)—Re(2)—Re(1) 115.21(2), P(1)—Re(2)—P(2) 164.84(3), C(4)—Re(1)—Re(2) 148.2(1), C(7)—Re(2)—Re(1) 149.2(1), C(1)—Re(1)—Re(2) 118.1(1), C(2)—Re(1)—C(3) 177.8(2), C(6)—Re(2)—C(5) 177.5(2), C(4)—Re(1)—C(1) 93.6(2), C(7)—Re(2)—P(2) 95.6(1), C(12)—P(1)—C(8) 103.0(2).

(iii) Reaction of [$Re_2(CO)_{10}$] with PTh_3: Carbon−Phosphorus Bond Cleavage

Since generation of a metal-bound thienyl moiety from a tri(2-thienyl)phosphine ligand is not achieved at moderate temperatures, for comparison with the work described above, we conducted the direct reaction of [$Re_2(CO)_{10}$] and PTh_3 at high temperature. In refluxing xylene, a complex mixture of products was obtained. These include the previously described binuclear complexes **3**–**5**, two new binuclear products, [$Re_2(CO)_7(PTh_3)(\mu\text{-}PTh_2)(\mu\text{-}\eta^1{:}\kappa^1\text{-}C_4H_3S)$] (**6**) and [$Re_2(CO)_7(\mu\text{-}\kappa^1{:}\kappa^2\text{-}Th_2PC_4H_2SPTh)(\mu\text{-}\eta^1{:}\kappa^1\text{-}C_4H_3S)$] (**7**), and the mononuclear hydrides [$HRe(CO)_4(PTh_3)$] (**8**) and *trans*-[$HRe(CO)_3(PTh_3)_2$] (**9**) (Scheme 3). Apparently only carbon−phosphorus bond cleavage has occurred and in all products the carbon−sulfur bonds remain intact.

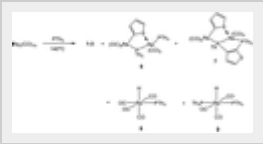

Scheme 3

Complex **6** is a substitution product of **4**. The $^{31}P\{^{1}H\}$ NMR spectrum shows two equal intensity doublets at δ −21.2 and −56.1 (J_{PP} = 98.2 Hz), and the FAB mass spectrum has a parent molecular ion at *m*/*z* 1130 together with fragmentation peaks due to the sequential loss of all seven carbonyl ligands. An ORTEP drawing of the molecular structure of **6** is depicted in Figure 4. The structure is similar to that of **4** except that an equatorial carbonyl group at one rhenium atom is replaced by a PTh_3 ligand. The Re···Re distance is very long [4.228(1) Å] and is clearly a nonbonding distance, and the rhenium−carbon bond [Re(1)—C(8) 2.173(4) Å] is similar to that observed in **B** (Chart 1) [2.160(11) Å].[23] Likewise, the rhenium−sulfur bond [Re(2)—S(1) 2.5101(11) Å] is similar to that in **B** and related complexes.[16-21,23]

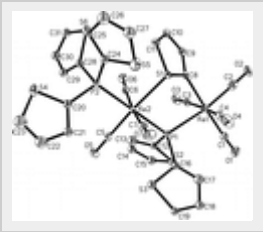

Figure 4. ORTEP diagram of the molecular structure of $[Re_2(CO)_7(PTh_3)(\mu\text{-}PTh_2)(\mu\text{-}\eta^1\text{:}\kappa^1\text{-}C_4H_3S)]$ (**6**), showing 50% probability thermal ellipsoids. Selected interatomic distances (Å) and angles (deg): Re(1)—C(8) 2.173(4), Re(1)—P(1) 2.525(1), Re(2)—P(2) 2.405(1), Re(2)—P(1) 2.485(1), Re(2)—S(1) 2.510(1), av Re—C 1.979(5), av C—O 1.133(6), C(2)—Re(1)—C(1) 91.6(2), C(4)—Re(1)—C(3) 170.6(2), C(2)—Re(1)—P(1) 171.7(2), C(8)—Re(1)—P(1) 85.9(1), C(7)—Re(2)—C(6) 172.0(2), P(2)—Re(2)—P(1) 178.35(4), C(5)—Re(2)—S(1) 174.7(1), P(2)—Re(2)—S(1) 94.76(4), P(1)—Re(2)—S(1) 85.64(4), C(11)—S(1)—Re(2) 112.7(2), C(8)—S(1)—Re(2) 105.9(2).

It was not possible to unambiguously assign a structure to **7** in the absence of an X-ray crystallographic study, the result of which is summarized in Figure 5. The molecule contains a very unusual $\mu\text{-}\kappa^1\text{:}\kappa^2\text{-}Th_2P(C_4H_2S)PTh$ ligand, which bridges the rhenium centers through one phosphorus atom, P(2), while Re(1) coordinates with the other phosphorus atom, P(1), thus forming a five-membered chelate ring. Overall, the molecule has four fused five-membered rings. The thienyl bridge is similar to that found in **6** and the rhenium−carbon [Re(2)—C(24) 2.188(4) Å] and rhenium−sulfur [Re(1)—S(5) 2.4918(11) Å] distance is similar. Each rhenium achieves an 18-electron configuration without a rhenium−rhenium bond, which is consistent with the long Re···Re distance of 4.217(1) Å. Spectroscopic data are consistent with the solid-state structure. The FAB mass spectrum shows a molecular ion at *m*/*z* 1046, and in the $^{31}P\{^{1}H\}$

NMR spectrum two doublets at δ −2.7 and −35.6 (J_{PP} = 11.4 Hz) are observed. The mode of formation of **7** remains unclear.

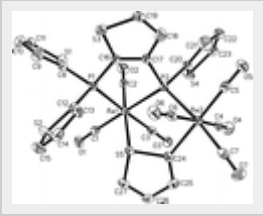

Figure 5. ORTEP diagram of the molecular structure of $[Re_2(CO)_7(\mu\text{-}\kappa^1\text{:}\kappa^2\text{-}Th_2PC_4H_2SPTh)(\mu\text{-}\eta^1\text{:}\kappa^1\text{-}C_4H_3S)]$ (**7**), showing 50% probability thermal ellipsoids. Selected interatomic distances (Å) and angles (deg): Re(2)—C(24) 2.188(4), Re(1)—P(1) 2.435(1), Re(1)—P(2) 2.489(1), Re(2)—P(2) 2.509(1), Re(1)—S(5) 2.492(1), av Re—C 1.965(5), av C—O 1.143(6), C(3)—Re(1)—P(1) 172.1(1), C(1)—Re(1)—P(1) 93.7(1), C(1)—Re(1)—P(2) 174.6(1), P(1)—Re(1)—P(2) 83.09(4), C(2)—Re(1)—S(5) 176.9(1), P(1)—Re(1)—S(5) 87.20(4), P(2)—Re(1)—S(5) 83.88(3), C(7)—Re(2)—C(5) 94.7(2), C(6)—Re(2)—C(4) 174.2(2), C(7)—Re(2)—P(2) 173.2(1), C(16)—P(1)—Re(1) 106.7(2), C(17)—P(2)—Re(1) 106.3(2), Re(1)—P(2)—Re(2) 115.09(4), C(27)—S(5)—Re(1) 109.9(2), C(24)—S(5)—Re(1) 106.2(2).

Two mononuclear hydrides, $[ReH(CO)_4(PTh_3)]$ (**8**) and *trans*-$[ReH(CO)_3(PTh_3)_2]$ (**9**), were also obtained from the reaction. The former was easily characterized by comparison of spectroscopic data with that of $[ReH(CO)_4(PPh_3)]$.[41] Importantly, in the ^{1}H NMR spectrum a high-field doublet was observed at δ −4.83 (J_{PH} = 25.5 Hz), indicating the presence of a terminal hydride, while the $^{31}P\{^1H\}$ NMR spectrum displayed only a singlet at δ −24.8, consistent with the proposed structure. The structure of *trans*-$[ReH(CO)_3(PTh_3)_2]$ (**9**) was confirmed by a crystallographic study, and the molecular structure is shown in Figure 6. The molecule contains two crystallographic planes of symmetry. The distorted octahedral rhenium atom binds three carbonyls in a *meridional*arrangement, two PTh_3 ligands, which lie *trans* to one another, and an axial hydride. Presumably, the phosphines lie *trans* to each other to minimize steric congestion, and the rhenium−phosphorus bond distance is 2.3690(17) Å. The structure is very similar to that of *trans*-$[ReH(CO)_3(PPh_3)_2]$.[42] The hydride ligand was not located in the structural analysis, presumably due to disorder, but the widening of the *cis*-C—Re—C angles and the reduction of *trans*-C—Re—C angles [168.0(8)°] suggest the presence of a hydride ligand in this position. This is also confirmed by the ^{1}H NMR spectrum of **9**, which shows a triplet at δ −4.57 (J = 20.8 Hz), indicating the presence of a terminal hydride coupled with two equivalent phosphorus atoms. The hydride ligand is shown in its calculated position in Figure 6. The $^{31}P\{^1H\}$ NMR spectrum consists of only a singlet at δ −19.9 ppm.

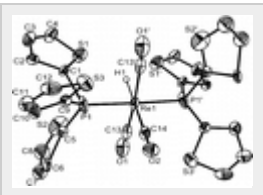

Figure 6. ORTEP diagram of the molecular structure of *trans*-[$HRe(CO)_3(PTh_3)_2$] (**9**), showing 50% probability thermal ellipsoids. Selected interatomic distances (Å) and angles (deg): Re(1)—P(1) 2.369(2), Re(1)—C(14) 2.00(1), Re(1)—C(13) 2.007(9), C(14)—Re(1)—C(13) 96.0(4), C(13)—Re(1)—C(13A) 168.0(8), C(14)—Re(1)—P(1) 91.0(3), C(13)—Re(1)—P(1) 89.3(2), C(13A)—Re(1)—P(1) 90.5(2), P(1A)—Re(1)—P(1) 178.0(6).

The precise mode of formation of hydrides **8** and **9** is unclear. Formation of *trans*-[$ReH(CO)_3(PPh_3)_2$] from $HRe(CO)_5$ and PPh_3 is extremely slow (10 days in refluxing xylene),[42] which suggests that **8** and **9** are formed via independent pathways. Hydrides [$HRe(CO)_4(PPh_3)$] and *trans*-[$HRe(CO)_3(PPh_3)_2$] are known products of the substitution of [$Re_2(CO)_{10}$] by PPh_3 at high temperatures.[43] Formation of all these hydrides may result from hydrogen abstraction reactions (probably from the solvent), which are accessible at very high temperatures.

(iv) Reaction of [$Mn_2(CO)_{10}$] with PTh_3: Phosphorus–Carbon Bond Cleavage

Since the behavior of PTh_3 with dirhenium complexes is quite different from that of Ph_2PTh, we also investigated the reactivity of PTh_3 with $Mn_2(CO)_{10}$. Deeming et al. reported formation of two dimanganese complexes, **C** and **D**, from the reaction between [$Mn_2(CO)_{10}$] and Ph_2PTh in refluxing xylene (Chart 1).[23] In contrast, we have obtained three dimanganese complexes, [$Mn_2(CO)_9(PTh_3)$] (**10**), [$Mn_2(CO)_6(\mu\text{-}PTh_2)(\mu\text{-}\eta^1\text{:}\eta^5\text{-}C_4H_3S)$] (**11**), and [$Mn_2(CO)_5(PTh_3)(\mu\text{-}PTh_2)(\mu\text{-}\eta^1\text{:}\eta^5\text{-}C_4H_3S)$] (**12**), in 13, 46, and 29% yields, respectively, from heating $Mn_2(CO)_{10}$ with PTh_3in toluene (Scheme 4). In a separate experiment we have shown that **11** is a precursor of **12**.

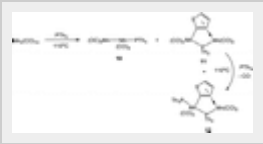

Scheme 4

Characterization of **10** was straightforwardly made by comparison with spectroscopic data for [$Mn_2(CO)_9L$] complexes.[23,31a] The IR spectra are all very similar, and the FAB mass spectrum showed a molecular ion at *m*/*z* 642. The ^1H NMR spectrum displays only aromatic resonances for the thienyl ring protons, while the $^{31}P\{^1H\}$ NMR spectrum consists of a singlet at δ 52.1.

Likewise, spectroscopic data for **11** are very similar to those previously noted for **D** (Chart 1). In addition to two broad singlets at δ 7.45 and 7.30 (each integrating to 3H), the ^1H NMR spectrum displays three upfield broad singlets at δ 6.19, 5.80, and 5.74, each integrating to one proton, indicative of π-complexation of a thienyl ring. The $^{31}P\{^1H\}$ NMR spectrum shows only a singlet at δ −51.5, and the FAB mass spectrum exhibits a parent molecular ion at *m*/*z* 558 and further ions

due to sequential loss of all carbonyls. A single-crystal X-ray structure was carried out, and the molecular structure of **11** is shown in Figure 7. The structure is very similar to that of **D**. The Mn···Mn distance is 3.510(1) Å, suggesting the absence of a direct metal−metal bond. With the phosphido bridge acting as a three-electron donor, the bridging thienyl ligand must donate a total of seven electrons to the dimanganese center. This interpretation is supported by the η^5-coordination mode of the thienyl ligand toward Mn(2) with manganese−carbon distances in the range 2.130(2)−2.198(2) Å, being longer than the σ manganese−carbon bond distance [Mn(1)—C(7) 2.077(2) Å]. The phosphido bridge binds asymmetrically [Mn(1)—P(1) 2.3681(6) and Mn(2)—P(1) 2.2777(6) Å], consistent with a net 18-electron configuration of each metal center. As a result, Mn(1) has an octahedral arrangement of ligands, while Mn(2) adopts a half-sandwich geometry. The η^1:η^5-thienyl ring is approximately planar except that the sulfur atom of the ring is −0.107(2) Å out of the plane of the four carbon atoms opposite to Mn(2), +1.732(2) Å. The NMR data show that the solid-state structure persists in solution.

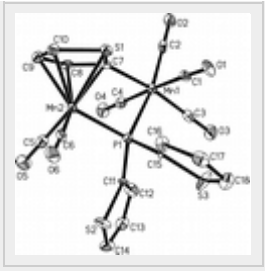

Figure 7. ORTEP diagram of the molecular structure of $[Mn_2(CO)_6(\mu\text{-}PTh_2)(\mu\text{-}\eta^1\text{:}\eta^5\text{-}C_4H_3S)]$ (**11**), showing 50% probability thermal ellipsoids. Selected interatomic distances (Å) and angles (deg): Mn(1)—P(1) 2.3681(6), Mn(2)—P(1) 2.2777(6), Mn(2)—S(1) 2.3056(6), Mn(1)—C(7) 2.077(2), Mn(2)—C(7) 2.198(2), Mn(2)—C(8) 2.179(2), Mn(2)—C(9) 2.153(2), Mn(2)—C(10) 2.130(2), C(3)—Mn(1)—C(2) 96.26(9), C(1)—Mn(1)—C(4) 177.06(9), C(3)—Mn(1)—C(7) 171.12(9), C(2)—Mn(1)—C(7) 92.48(8), C(3)—Mn(1)—P(1) 95.72(7), C(2)—Mn(1)—P(1) 167.77(7), C(7)—Mn(1)—P(1) 75.63(5), C(1)—Mn(1)—P(1) 86.83(7), C(1)—Mn(1)—C(7) 93.08(8), C(5)—Mn(2)—P(1) 93.77(7), C(6)—Mn(2)—P(1) 98.95(7), C(7)—Mn(2)—P(1) 75.31(5), Mn(2)—P(1)—Mn(1) 98.14(2), Mn(1)—C(7)—Mn(2) 110.34(9), C(15)—P(1)—C(11) 101.6(6).

An ORTEP diagram of the molecular structure of **12** is shown in Figure 8. The molecule consists of a dimanganese core [Mn(1)···Mn(2) 3.479(1) Å] coordinated by five terminal carbonyl ligands, a terminal tri(2-thienyl)phosphine ligand, and bridging thienyl and di(2-thienyl)phosphide ligands. It is the tri(2-thienyl)phosphine derivative of **11**, the equatorial carbonyl ligand on Mn(1) *trans* to the phosphido bridge being replaced by a tri(2-thienyl)phosphine ligand. Like **11**, the ^{1}H NMR spectrum of **12** displays three upfield broad singlets at δ 5.82, 5.63, and 5.51 (each integrating to 1H) due the π-complexed thienyl ring, and the $^{31}P\{^1H\}$ NMR spectrum displays two singlets at δ 45.6 and −30.3. The FAB mass spectrum shows a parent molecular ion at *m*/*z* 810 and peaks due to stepwise loss of five carbonyl groups, which is consistent with the solid-state structure.

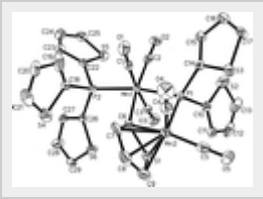

Figure 8. ORTEP diagram of the molecular structure of $[Mn_2(CO)_5(PTh_3)(\mu\text{-}PTh_2)(\mu\text{-}\eta^1\text{:}\eta^5\text{-}C_4H_3S)]$ (**12**), showing 50% probability thermal ellipsoids. Selected interatomic distances (Å) and angles (deg): Mn(1)—P(1) 2.3416(7), Mn(1)—P(2) 2.2824(7), Mn(2)—P(1) 2.2762(7), Mn(2)—S(1) 2.3020(8), Mn(1)—C(6) 2.093(2), Mn(2)—C(6) 2.185(2), Mn(2)—C(7) 2.178(3), Mn(2)—C(8) 2.154(3), Mn(2)—C(9) 2.123(3), C(1)—Mn(1)—C(3) 175.1(1), C(2)—Mn(1)—C(6) 171.3(1), C(2)—Mn(1)—P(2) 98.89(8), C(6)—Mn(1)—P(2) 89.70(7), C(6)—Mn(1)—P(1) 75.93(7), P(2)—Mn(1)—P(1) 165.02(3), C(1)—Mn(1)—P(1) 84.14(7), C(1)—Mn(1)—P(2) 91.87(7), C(1)—Mn(1)—C(6) 90.4(1), C(4)—Mn(2)—C(5) 90.7(1), C(4)—Mn(2)—P(1) 93.75(8), C(5)—Mn(2)—P(1) 97.65(9), Mn(2)—P(1)—Mn(1) 97.76(3), Mn(1)—C(6)—Mn(2) 108.8(1), C(10)—P(1)—C(14) 98.2(8).

Conclusions

The present study has demonstrated that only carbon−phosphorus bond cleavage of the PTh_3ligand occurs at high temperatures at both the dirhenium and dimanganese centers. In the case of dirhenium complexes, simple mono- and disubstituted products **1**−**3** are obtained at moderate temperature, with **2** showing a rare example of two different substituents being bound to the same metal atom in a disubstituted $[Re_2(CO)_{10}]$ derivative. At higher temperatures, transformations of **1**and **3** into **4** and **5**, respectively, represent dirhenium-promoted carbon−phosphorus bond cleavage of a coordinated PTh_3 ligand. In contrast to Ph_2PTh,[23] PTh_3 has proved to be a versatile synthon for a variety of mono- and dinuclear complexes when reacted with dirhenium complexes at different conditions. In complexes **4**, **6**, and **7**, a thienyl ligand bridges the dirhenium unit, being coordinated via sulfur and carbon atoms (next to sulfur). Another interesting finding is the carbon−phosphorus coupling observed in **7** resulting in the formation of a novel $\mu\text{-}\kappa^1\text{:}\kappa^2\text{-}Th_2PC_4H_2SPTh$ ligand. Three hydrides have been prepared. Mononuclear **8** and **9** each contain a terminal hydride, and in **5** it bridges the rhenium−rhenium bond. These are likely formed via high-temperature hydrogen abstraction reactions. Interestingly, the reaction of $[Mn_2(CO)_{10}]$ with tri(2-thienyl)phosphine furnishes **11** and **12** as a result of carbon−phosphorus bond activation. Each contains a bridging thienyl ligand bound to one manganese atom in a η^5-coordination mode. This observation parallels that reported for Ph_2PTh.[23] In the present work we have not been able to isolate any complexes resulting from carbon−sulfur bond cleavage of the tri(2-thienyl)phosphine ligand or indeed the thienyl ligand generated from this.

Experimental Section

All reactions were carried out under a nitrogen atmosphere using standard Schlenk techniques unless otherwise stated. Reagent-grade solvents were dried using appropriate drying agents and distilled by standard methods prior to use. Infrared spectra were recorded on a Shimadzu FTIR 8101 spectrophotometer. NMR spectra were recorded on Bruker DPX 400 and Varian Inova 500 instruments. Elemental analyses were performed by Microanalytical Laboratories, University College London. Fast atom bombardment mass spectra were obtained on a JEOLSX-102 spectrometer using 3-nitrobenzyl alcohol as matrix and CsI as calibrant. $[Re_2(CO)_{10}]$ and $[Mn_2(CO)_{10}]$ were purchased from Strem Chemicals Inc. and used as received. $Me_3NO{\cdot}2H_2O$ was purchased from Lancaster, water was removed using a Dean−Stark apparatus by azeotropic distillation from benzene, and the anhydrous Me_3NO was stored under nitrogen. PTh_3 was purchased from E. Merck and used as received. The compounds $[Re_2(CO)_9(NCMe)]$ and $[Re_2(CO)_8(NCMe)_2]$ were prepared according to literature methods.[29]

Reaction of $[Re_2(CO)_9(NCMe)]$ with PTh_3

A solution of $[Re_2(CO)_9(NCMe)]$ (250 mg, 0.375 mmol) and PTh_3 (105 mg, 0.374 mmol) in cyclohexane (20 mL) was heated to reflux for 1 h. The solvent was removed under reduced pressure and the residue separated by TLC on silica gel. Elution with hexane/CH_2Cl_2 (5:2, v/v) developed three bands, which gave the following compounds in order of elution: $[Re_2(CO)_9(PTh_3)]$ (**1**) (95 mg, 28%), $[Re_2(CO)_8(PTh_3)_2]$ (**3**) (95 mg, 22%) as pale yellow crystals, and $[Re_2(CO)_8(NCMe)(PTh_3)]$ (**2**) (148 mg, 43%) as colorless crystals after recrystallization from hexane/CH_2Cl_2 at 4 °C. Spectral data for **1**: Anal. Calcd for $C_{21}H_9O_9P_1Re_2S_3$: C, 27.87; H, 1.00. Found: C, 28.13; H, 1.25. IR (ν(CO), CH_2Cl_2): 2107 s, 2037 m, 1998 vs, 1963 s, 1943 s cm^{-1}. ^1H NMR ($CDCl_3$): δ 7.64 (m, 3H), 7.35 (m, 3H), 7.22 (m, 3H). $^{31}P\{^1H\}$ NMR ($CDCl_3$): δ −24.5 (s). MS (FAB): *m*/*z* 904 (M^+). Spectral data for **2**: Anal. Calcd for $C_{22}H_{12}N_1O_8P_1Re_2S_3$: C, 28.79; H, 1.32. Found: C, 29.05; H, 1.73. IR (ν(CO), CH_2Cl_2): 2087 s, 2002 m, 1977 vs, 1949 m, 1917 m cm^{-1}. ^1H NMR ($CDCl_3$): δ 7.60 (m, 3H), 7.42 (m, 3H), 7.19 (m, 3H), 2.0 (s, 3H). $^{31}P\{^1H\}$ NMR ($CDCl_3$): δ −23.6 (s). MS (FAB): *m*/*z* 917 (M^+). Spectral data for **3**: Anal. Calcd for $C_{32}H_{18}O_8P_2Re_2S_6$: C, 33.21; H, 1.57. Found: C, 33.42; H, 1.75. IR (ν(CO), CH_2Cl_2): 2017 w, 1991 sh, 1964 vs cm^{-1}. ^1H NMR ($CDCl_3$): δ 7.61 (m, 6H), 7.37 (m, 6H), 7.20 (m, 6H). $^{31}P\{^1H\}$ NMR ($CDCl_3$): δ −23.5 (s). MS (FAB): *m*/*z* 1158 (M^+).

Reaction of 1 with MeCN

To a CH_2Cl_2 solution (10 mL) of **1** (50 mg, 0.063 mmol) containing MeCN (5 mL) was added a solution of Me_3NO in methanol (ca. 0.10 mg/mL) by means of a dropping funnel (ca. 0.2 mL), and the reaction mixture was stirred at room temperature for 2 h. Complete consumption of **1** was confirmed by TLC monitoring. The reaction mixture was then passed through a silica column (4 cm) to remove excess Me_3NO. The solvent was removed under reduced pressure and the residue recrystallized from hexane/CH_2Cl_2 to give **2** (26 mg, 51%).

Reaction of 2 with Tri(2-thienyl)phosphine

A CH_2Cl_2 solution (20 mL) of **2** (100 mg, 0.108 mmol) and $P(C_4H_3S)_3$ (65 mg, 0.232 mmol) was stirred for 2 h at 25 °C. The solvent was evaporated to dryness, and the residue chromatographed by TLC on silica gel. Elution with hexane/CH_2Cl_2 (5:2, v/v) developed only one band, which gave **3**(110 mg, 62%).

Reaction of $[Re_2(CO)_{10}(NCMe)_2]$ with PTh_3

To a CH_2Cl_2 solution (20 mL) of $[Re_2(CO)_{10}(NCMe)_2]$ (ca. 150 mg, 0.221 mmol) was added PTh_3(63 mg, 0.225 mmol), and the reaction mixture was stirred at room temperature for 2 h, during which time the color of the reaction mixture changed from pale yellow to colorless. The solvent was evaporated to dryness, and the residue was chromatographed by TLC on silica gel. Elution with hexane/CH_2Cl_2 (5:2, v/v) developed two bands, which gave **3** (41 mg, 16%) and **2** (124 mg, 61%) in order of elution.

Thermolysis of 1

A xylene solution (25 mL) of **1** (50 mg, 0.063 mmol) was refluxed for 6 h. A similar chromatographic separation to that above developed two bands. The minor band was unreacted **1**(10 mg, 15%). The major band gave $[Re_2(CO)_8(\mu\text{-}PTh_2)(\mu\text{-}\eta^1\text{:}\kappa^1\text{-}C_4H_3S)]$ (**4**) as colorless crystals (70 mg, 35%) after recrystallization from hexane/CH_2Cl_2 by slow evaporation of the solvents. Spectral data for **4**: Anal. Calcd for $C_{27}H_{19}O_3P_2Re_1S_6$: C, 27.39; H, 1.03. Found: C, 28.25; H, 1.30. IR (ν(CO), CH_2Cl_2): 2106 w, 2086 s, 2015 vs, 1994 s, 1979 s, 1968 s, 1948 m cm^{-1}. ^1H NMR ($CDCl_3$): δ 7.72 (m, 1H), 7.50 (m, 2H), 7.34 (m, 2H), 7.09 (m, 4H). $^{31}P\{^1H\}$ NMR ($CDCl_3$): δ −58.2 (s). $^{13}C\{^1H\}$ NMR: δ 168.4 (s), 146.2 (s), 146.0 (s), 140.9 (d, *J* = 4.8 Hz), 135.6 (s), 134.4 (d, *J* = 8.7 Hz), 133.2 (d, *J* = 4.3 Hz), 130.7 (d, *J* = 1.9 Hz), 127.9 (d, *J* = 9.2 Hz) (*ipso* and CO signals unobserved). MS (FAB): *m*/*z* 876 (M^+).

Thermolysis of 3

A xylene (15 mL) solution of **3** (40 mg, 0.034 mmol) was refluxed under nitrogen for 4 h. A similar chromatographic separation to that above gave two bands. The minor band was unreacted starting material (12 mg, 30%). The major band gave $[Re_2(CO)_7(PTh_3)(\mu\text{-}PTh_2)(\mu\text{-}H)]$ (**5**) as colorless crystals (18 mg, 50%) after recrystallization from hexane/CH_2Cl_2 at 25 °C. Spectral data for **5**: Anal. Calcd for $C_{27}H_{16}O_7P_2Re_2S_5$: C, 30.97; H, 1.54. Found: C, 31.21; H, 1.85. IR (ν(CO), CH_2Cl_2): 2096 m, 2050 w, 2000 vs, 1952 s, 1930 m cm^{-1}. ^1H NMR ($CDCl_3$): δ 7.64 (m, 3H), 7.42 (m, 7H), 7.21 (m, 3H), 7.02 (m, 2H), −13.83 (dd, *J* = 16.4, 5.2 Hz, 1H). $^{31}P\{^1H\}$ NMR ($CDCl_3$): δ −8.3 (d, *J* = 75.8 Hz, 1P) and −28.4 (d, *J* = 75.8 Hz, 1P). MS (FAB): *m*/*z* 1048 (M^+).

Reaction of $[Re_2(CO)_{10}]$ with PTh_3

A xylene (30 mL) solution of $Re_2(CO)_{10}$ (300 mg, 0.46 mmol) and PTh_3 (256 mg, 0.913 mmol) was refluxed for 7 h. Workup and chromatographic separation as above developed seven bands, which afforded the following compounds in order of elution: **5** (96 mg, 20%), $[HRe(CO)_4(PTh_3)]$ (**8**) as colorless crystals (16 mg, 3%), $[HRe(CO)_3(PTh_3)_2]$ (**9**) as colorless crystals (38 mg, 5%), **4**(101 mg, 25%), $[Re_2(CO)_7(\mu\text{-}\kappa^1\text{:}\kappa^2\text{-}Th_2PC_4H_2SPTh)(\mu\text{-}\eta^1\text{:}\kappa^1\text{-}C_4H_3S)]$ (**7**) as pale yellow crystals (38 mg, 8%), **3** (16 mg, 3%), and $[Re_2(CO)_7(PTh_3)(\mu\text{-}PTh_2)(\mu\text{-}\eta^1\text{:}\kappa^1\text{-}C_4H_3S)]$ (**6**) as pale yellow crystals (156 mg, 30%) from hexane/CH_2Cl_2 at 25 °C. Spectral data for **6**: Anal. Calcd for $C_{31}H_{18}O_7P_2Re_2S_6$: C, 32.97; H, 1.61. Found: C, 33.15; H, 1.96. IR (ν(CO), CH_2Cl_2): 2085 m, 2058 w, 1991 vs, 1978 vs, 1964 vs, 1942 s cm^{-1}. ^1H NMR ($CDCl_3$, 300 K, 300 MHz): δ 7.66 (m, 2H), 7.61 (d, 1H, *J* = 4.2 Hz), 7.47 (m, 4H), 7.38 (m, 3H), 7.20 (m, 4H), 7.06 (m, 2H), 6.90 (m, 1H), 6.37 (d, 1H, *J* = 4.2 Hz). $^{31}P\{^1H\}$ NMR ($CDCl_3$): δ −21.2 (d, *J* = 98.2 Hz, 1P), −56.1 (d, *J* = 98.2 Hz, 1P). MS (FAB): *m*/*z* 1130 (M^+). Spectral data for **7**: Anal. Calcd for $C_{27}H_{14}O_7P_2Re_2S_5$: C, 31.03; H, 1.35. Found: C, 31.95; H, 1.85. IR (ν(CO), CH_2Cl_2): 2086 m, 2056 w, 2034 vs, 1986 vs, 1955 s, 1941 vs cm^{-1}. ^1H NMR ($CDCl_3$, 298 K, 500 MHz): δ 8.32 (d, *J* = 5.5 Hz, 1H), 7.72 (m, 1H), 7.63 (m, 1H), 7.60 (m, 2H), 7.49 (d, *J* = 5.5 Hz, 1H), 7.42 (m, 1H), 7.31 (m, 1H), 7.20 (m, 2H), 7.13 (m, 1H), 7.07 (m, 2H), 6.97 (m, 1H). $^{31}P\{^1H\}$ NMR ($CDCl_3$): δ −2.7 (d, *J* = 11.4 Hz, 1P), −35.6 (d, *J*= 11.4 Hz, 1P). MS (FAB): *m*/*z* 1046 (M^+). Spectral data for **8**: Anal. Calcd for $C_{16}H_{10}O_4P_1Re_1S_3$: C, 33.15; H, 1.74. Found: C, 34.15; H, 1.95. IR (ν(CO), CH_2Cl_2): 2106 m, 2086 s, 2015 vs, 1996 vs, 1967 vs, 1947 s cm^{-1}. ^1H NMR ($CDCl_3$): δ 7.5 (m, 3H), 7.38 (m, 3H), 7.27 (m, 3H), −4.83 (d, *J*= 25.5 Hz, 1H). $^{31}P\{^1H\}$ NMR ($CDCl_3$): δ −24.8 (s). MS (FAB): *m*/*z* 800 (M^+). Spectral data for **9**: Anal. Calcd for $C_{27}H_{19}O_3P_2Re_1S_6$: C, 38.98; H, 2.30. Found: C, 39.25; H, 2.45. IR (ν(CO), CH_2Cl_2): 1960 m, 1941 br, 1928 sh cm^{-1}. ^1H NMR ($CDCl_3$): δ 7.5 (m, 6H), 7.38 (m, 6H), 7.27 (m, 6H), −4.57 (t, *J* = 20.8 Hz, 1H). $^{31}P\{^1H\}$ NMR ($CDCl_3$): δ −19.9 (s). MS (FAB): *m*/*z* 832 (M^+).

Reaction of $[Mn_2(CO)_{10}]$ with PTh_3

To a toluene solution (20 mL) of $[Mn_2(CO)_{10}]$ (115 mg, 0.294 mmol) was added PTh_3 (85 mg, 0.303 mmol), and the reaction mixture was heated to reflux for 5 h. The solvent was removed under reduced pressure and the residue chromatographed by TLC on silica gel. Elution with hexane/CH_2Cl_2 (4:1, v/v) afforded five bands. The first band afforded unreacted $Mn_2(CO)_{10}$(trace). The second band yielded $[Mn_2(CO)_9(PTh_3)]$ (**10**) (25 mg, 13%) as yellow crystals from hexane/CH_2Cl_2 at 4 °C. The third band was too small for complete characterization. The fourth and fifth bands gave $[Mn_2(CO)_6(\mu\text{-}PTh_2)(\mu\text{-}\eta^1\text{:}\eta^5\text{-}C_4H_3S)]$ (**11**) (76 mg, 46%) and $[Mn_2(CO)_5(PTh_3)(\mu\text{-}PTh_2)(\mu\text{-}\eta^1\text{:}\eta^5\text{-}C_4H_3S)]$ (**12**) (70 mg, 29%), respectively, as orange crystals after recrystallization from hexane/CH_2Cl_2 at 4 °C. Analytical and spectroscopic data for **10**: Anal. Calcd for $C_{21}H_9Mn_2O_9PS_3$: C, 39.27; H, 1.41. Found: C, 39.42; H, 1.55. IR (ν(CO), CH_2Cl_2): 2092 m, 2015 s, 1997 vs, 1975 s, 1965 w cm^{-1}. ^1H NMR ($CDCl_3$): δ 7.60 (m, 3H), 7.25 (m, 3H), 7.05 (m, 3H). $^{31}P\{^1H\}$ NMR ($CDCl_3$): δ 52.1 (s). MS (FAB): *m/z* 642 $(M)^+$. Analytical and spectroscopic data for **11**: Anal. Calcd for $C_{18}H_9Mn_2O_6PS_3$: C, 38.32; H, 1.62. Found: C, 38.48; H, 1.78. IR (ν(CO), CH_2Cl_2): 2069 m, 1994 s, 1981 vs, 1974 s, 1963 s, 1926 s cm^{-1}. ^1H NMR ($CDCl_3$): δ 7.40 (bs, 3H), 7.30 (bs, 3H), 6.19 (bs, 1H), 5.80 (bs, 1H), 5.74 (bs, 1H). $^{31}P\{^1H\}$ NMR ($CDCl_3$): δ −51.5 (s). MS (FAB): *m/z* 558 $(M)^+$. Analytical and spectroscopic data for **12**: Anal. Calcd for $C_{29}H_{18}Mn_2O_5P_2S_6$: C, 42.97; H, 2.01. Found: C, 43.19; H, 2.16. IR (ν(CO), CH_2Cl_2): 2040 w, 1994 w, 1968 vs, 1940 vs, 1918 s cm^{-1}. ^1H NMR ($CDCl_3$): δ 7.48−6.69 (m, 15H), 5.82 (bs, 1H), 5.63 (bs, 1H), 5.51 (bs, 1H). $^{31}P\{^1H\}$ NMR ($CDCl_3$): δ 45.6 (s), −30.3 (s). MS (FAB): *m/z* 810 $(M)^+$.

X-ray Structure Determinations

Single crystals of compounds **2**, **3**, **5**, **6**, **7**, **9**, **11**, and **12** suitable for X-ray diffraction were obtained by recrystallization from hexane/CH_2Cl_2 at room temperature and mounted on Nylon fibers with mineral oil, and diffraction data were collected at 150(2) K on a Bruker AXS SMART diffractometer equipped with an APEX CCD detector using graphite-monochromated Mo Kα radiation (λ = 0.71073 Å). Integration of intensities and data reduction was performed using the SAINT program.[44] Multiscan absorption correction was applied using the SADABS procedure.[45] The structures were solved by direct methods(46) and refined by full-matrix least-squares on F^2.[47] All non-hydrogen atoms were refined anisotropically.

Acknowledgment

M.N.U. thanks Hajee Mohammad Danesh Science and Technology University for study leave to work at Jahangirnagar University. N.B. thanks Sher-e-Bangla Agricultural University for leave to

work at Lund University. This research has been sponsored by the Swedish Research Council (VR), the Royal Swedish Academy of Sciences, and the Swedish International Development Agency (SIDA).

References

[1]Topsøe, H., Clausen, B. A., and Massoth, F. E. *Hydrotreating Catalysis*; Springer: Berlin, **1996**.

[2]*Petroleum Chemistry and Refining*; Speight, J. G., Ed.; Taylor & Francis: Washington, DC, **1998**.

[3]*Geochemistry of Sulfur in Fossil Fuels*; Orr, W. L. and White, C. M., Eds.; ACS Symposium Series 429;American Chemical Society: Washington, DC, **1990**.

[4]Angelici, R. J. In *Encyclopedia of Inorganic Chemistry*; King, R. B., Ed.; Wiley: New York, **1994**; Vol. 3, pp1433− 1443.

[5]Whitehurst, D. D.; Isoda, T.; Mochida, I. *Adv. Catal.* **1998**, 42, 345

[6]Gates, B. C.; Katzer, J. R.; Schuit, G. C. A. *Chemistry of Catalytic Processes*; McGraw-Hill: New York,**1979**; pp 390− 447. (b) Galpern, G. D. In *The Chemistry of Heterocyclic Compounds*; Gronowitz, S., Ed.; Wiley: New York, **1985**, : Vol. 44, Part 1, pp 325− 351.

[7]Ledoux, M. J.; Michaux, O.; Agostini, G.; Panissod, P. *J. Catal.* **1986**, 102, 275

[8]Pecoraro, T. A.; Chianelli, R. R. *J. Catal.* **1981**, 67, 430 (b) Chianelli, R. R.*Catal. Rev.* **1984**, 26, 361

[9]Sanchez-Delgado, R. A. *J. Mol. Catal.* **1994**, 86, 287 (b) Angelici, R. J.*Polyhedron* **1997**, 16, 3073 (c) Bianchini, C.; Meli, A. *J. Chem. Soc., Dalton Trans.* **1996**, 801

[10]Bianchini, C.; Meli, A. *Acc. Chem. Res.* **1998**, 31, 109 (b)Rauchfuss, T. B. *Prog. Inorg. Chem.* **1991**, 39, 259 (c) Vicic, D. A.; Jones, W. D. *J. Am. Chem. Soc.* **1999**, 121, 7606

[11]Angelici, R. J. *Acc. Chem. Res.* **1988**, 21, 387 (b) Sauer, N. N.;Angelici, R. J. *J. Catal.* **1989**, 116, 11 (c) Garcia, J. J.; Mann, B. E.; Adams, H.;Bailey, N. A.; Maitlis, P. M. *J. Am. Chem. Soc.* **1995**, 117, 2179

[12]Brorson, M.; King, J. D.; Kiriakidou, K.; Prestopino, F.; Nordlander, E. *Metal Clusters in Chemistry*;Braunstein, P.; Oro, L. A.; Raithby, P. R., Eds.; Wiley-VCH: Weinheim, **1999**; Vol. 2, Chapter 2.6, pp 741−781.

[13]Angelici, R. J. *Organometallics* **2001**, 20, 1259, and references therein

[14]Angelici, R. J. *Coord. Chem. Rev.* **1990**, 105, 61 (b) Angelici, R. J. *Coord. Chem. Rev.* **2000**, 206−207, 63

[15]Angelici, R. J. *Transition Met. Sulphides, NATO ASI Ser. 3* **1998**, 60, 89 (b)Bianchini, C.; Meli, A. *Transition Met. Sulphides, NATO ASI Ser. 3* **1998**, 60, 129 (c)Angelici, R. J. *Bull. Soc. Chim. Belg.* **1995**, 104, 265

[16]Reynolds, M. A.; Guzei, I. A.; Angelici, R. J. *J. Am. Chem. Soc.* **2002**, 124, 1689 (b) Reynolds, M. A.; Guzei, I. A.; Angelici, R. J. *Organometallics* **2001**, 20, 1071

[17]Vecchi, P. A.; Ellern, A.; Anjelici, R. J. *Organometallics* **2005**, 24, 2168 (b) Vecchi, P. A.; Ellern, A.; Anjelici, R. J. *J. Am. Chem. Soc.* **2003**, 125, 2064

[18]Li, H.; Yu, K.; Watson, E. J.; Virkaitis, K. L.; D'Acchioli, J. S.; Carpenter, G. B.; Sweigart, D. A.*Organometallics* **2002**, 21, 1262

[19]Hernández-Maldonado, A. J.; Yang, R. T. *J. Am. Chem. Soc.* **2004**, 126, 992

[20]Palmer, M. S.; Harris, S. *Organometallics* **2000**, 19, 2114

[21]Churchill, D. G.; Bridgewater, B. M.; Parkin, G. *J. Am. Chem. Soc.* **2000**, 122, 178

[22]King, J. D.; Monari, M.; Nordlander, E. *J. Organomet. Chem.* **1999**, 573, 272

[23]Deeming, A. J.; Shinhmar, M. K.; Arce, A. J.; Sanctis, Y. D. *J. Chem. Soc., Dalton Trans.* **1999**,1153

[24]Deeming, A. J.; Jayasuriya, S. N.; Arce, A. J.; Sanctis, Y. D. *Organometallics* **1996**, 15, 786

[25]Kazemifar, N. K. K.; Stchedroff, M. J.; Mottalib, M. A.; Selva, S.; Monari, M.; Nordlander, E. *Eur. J. Inorg. Chem.* **2006**, 2058 (b) Mottalib, M. A.; Kabir, S. E.; Tocher, D. A.;Deeming, A. J.; Nordlander, E. *J. Organomet. Chem.* **2007**, 692, 5007

[26]Bodensiek, U.; Vahrenkamp, H.; Rheinwald, G.; Stoeckli-Evans, H. *J. Organomet. Chem.* **1995**, 488,85

[27]Uddin, Md. N.; Begum, N.; Hassan, M. R.; Hogarth, G.; Kabir, S. E.; Miah, Md. A.; Nordlander, E.;Tocher, D. A. *J. Chem. Soc., Dalton Trans.* **2008**, 6219

[28]Bieger, K.; Estevan, F.; Lahuerta, P.; Lloret, J.; Pérez-Prieto, J.; Sanaú, M.; Siguero, N.; Stiriba, S.-E.*Organometallics* **2003**, 22, 1799 (b) Lloret, J.; Estevan, F.; Lahuerta, P.;Hirva, P.; Pérez-Prieto, J.; Sanaú, M. *Organometallics* **2006**, 25, 3156

[29]Ingham, W. L.; Coville, N. J. *J. Organomet. Chem.* **1992**, 423, 51

[30]Adams, R. D.; Belinski, J. A.; Schierlmann *J. Am. Chem. Soc.* **1991**, 113, 9004

[31]Koelle, U. *J. Organomet. Chem.* **1978**, 155, 53 (b) Harris, G. W.;Boeyens, J. C. A.; Coville, N. J. *J. Chem. Soc., Dalton Trans.* **1985**, 2277 (c)Grad, D. R.; Brown, T. L. *J. Am. Chem. Soc.* **1982**, 104, 6340

[32]Prest, D. W.; Mays, M. J.; Raithby, P. R. *J. Chem. Soc., Dalton Trans.* **1982**, 737

[33]Kabir, S. E.; Ahmed, F.; Ghosh, S.; Hassan, M. R.; Islam, M. S.; Sharmin, A.; Tocher, D. A.; Haworth, D. T.;Lindeman, S. V.; Siddiquee, T. A.; Bennett, D. W. *J. Organomet. Chem.* **2008**, 693, 2657

[34]Das, A.K.; Bulak, E.; Sarkar, B.; Lissner, F.; Schleid, T.; Niemeyer, M.; Fiedler, F.; Kaim, W. *Organometallics***2008**, 27, 218

[35]Kabir, S. E.; Ahmed, F.; Das, A.; Hassan, M. R.; Haworth, D. T.; Lindeman, S. V.; Siddiquee, T. A.;Bennett, D. W. *J. Organomet. Chem.* **2008**, 693, 1696

[36]Kabir, S. E.; Ahmed, F.; Das, A.; Hassan, M. R.; Haworth, D. T.; Lindeman, S. V.; Hossain, G. M. G.;Siddiquee, T. A.; Bennett, D. W. *J. Organomet. Chem.* **2007**, 692, 4337

[37]Machado, R. A.; Rivillo, D.; Arce, A. J.; D'Ornelas, L.; Sanctis, Y. D.; Atencio, R.; González, T.; Galarza, E. *J. Organomet. Chem.* **2004**, 689, 2486

[38]Machado, R. A.; Goite, M. C.; Rivillo, D.; Sanctis, Y. D.; Arce, A. J.; Deeming, A. J.; D'Ornelas, L.;Sierralta, A.; Atencio, R.; González, T.; Galarza, E. *J. Organomet. Chem.* **2007**, 692, 894

[39]Singleton, E.; Moelwyn-Hughes, J. T.; Garner, A.W. B. *J. Organomet. Chem.* **1970**, 21, 449

[40]Haupt, H. J.; Balsaa, P.; Flörke, U. *Inorg. Chem.* **1988**, 27, 280

[41]Flitcroft, N.; Leach, J. M.; Hopton, F. J. *J. Inorg. Nuc. Chem.* **1970**, 32, 137

[42]Flörke, U.; Haupt, H. J. *Zeit. Kristallogr.* **1992**, 201, 317

[43]Cox, D. J.; Davis, R. *J. Organomet. Chem.* **1980**, 186, 339

[44]*SAINT* software for CCD diffractometer, V.7.23A; Bruker AXS, **2005**.

[45]Sheldrick, G. M. *SADB 5*, Program for empirical absorption correction of area-detector data; Institüt für Anorganische Chemie der Universität, Göttingen: Germany, **1996**.

[46]Program XS from *SHELXTL* package, V. 6.12; Bruker AXS, **2001**.

[47]Program XL from *SHELXTL* package, V. 6.10; Bruker AXS, **2001**.